

Ozone pretreatment alleviates ischemia—reperfusion injury-induced myocardial ferroptosis by activating the Nrf2/Slc7a11/Gpx4 axis

Shengyang Ding¹, Xinyu Duanmu¹, Lingshan Xu, Liang Zhu^{*,2}, Zhouquan Wu^{*,2}

Department of Anesthesiology, the Affiliated Changzhou No 2 People's Hospital of Nanjing Medical University, Changzhou 213100, Jiangsu, China

ARTICLE INFO

Keywords:

Ozone
Ferroptosis
Oxidative stress
Ischemia-reperfusion injury
Myocardial protection
Mechanisms

ABSTRACT

Myocardial ischemia—reperfusion injury (MIRI) is defined as the additional damage that occurs during the process of restoring blood flow to the heart tissue after ischemia-induced damage. Ozone is a powerful oxidizer, but low concentrations of ozone can protect various organs from oxidative stress. Some studies have demonstrated a link between ozone and cardioprotection, but the mechanism remains unclear. To establish an in vivo animal model of ischemia—reperfusion injury (I/R), this study utilized C57 mice, while an in vitro model of hypoxia-reoxygenation (H/R) injury was developed using H9c2 cardiomyocytes to simulate ischemia—reperfusion injury. Ozone pretreatment was used in in vitro and in vivo experiments. Through this research, we found that ozone therapy can reduce myocardial injury, and further studies found that ozone regulates the expression levels of these ferroptosis-related proteins and transcription factors in the H/R model, which were screened by bioinformatics. In particular, nuclear translocation of Nrf2 was enhanced by pretreatment with ozone, inhibited ferroptosis and ameliorated oxidative stress by initiating the expression of Slc7a11 and Gpx4. Significantly, Nrf2 gene silencing reverses the protective effects of ozone in the H/R model. In summary, our results suggest that ozone protects the myocardium from I/R damage through the Nrf2/Slc7a11/Gpx4 signaling pathway, highlighting the potential of ozone as a new coronary artery disease therapy.

1. Introduction

Frequently occurring during cardiopulmonary bypass surgery, a pathophysiological process named myocardial ischemia reperfusion injury (MIRI) can cause cardiac insufficiency, including myocardial systolic function weakening, decreased coronary flow and changes in vascular reactivity. Abundant intricate factors could be the trigger of MIRI, encompassing increased reactive oxygen species (ROS), oxidative stress damage [1], inflammation [2], intracellular calcium overload [3], and impaired mitochondrial dysfunction [4]. Li et al. showed that ferroptosis is the most notable driving factor for the final infarct size [5]. In addition, ferroptosis may induce myocardial ischemia reperfusion injury through oxidative stress [6]. Therefore, to improve the prognosis after cardiopulmonary bypass surgery, it is necessary to elucidate the mechanism of MIRI for developing novel therapeutic strategies.

Consisting of three oxygen atoms, ozone is a colorless and unpleasant gas. Scientific evidence has shown that the influences on ozone are dose dependent: a high concentration of ozone induces severe oxidative

stress, leading to inflammatory responses and tissue damage, while a low concentration of ozone induces moderate oxidation and activates antioxidant pathways [7]. Ozone pretreatment is performed by giving a certain amount of a mixture of ozone and oxygen to the body cavity or circulatory system before insults [8]. Many similar experimental studies have also shown that ozone preconditioning can enhance the capacity of the antioxidant system and reduce the level of oxidative stress in the body by promoting the expression of downstream antioxidant proteins of Nrf2, thus protecting myocardial tissue from damage caused by ischemia—reperfusion [9–11]. However, the effect of ozone on myocardial ferroptosis is unclear to date.

As a recently discovered cell death mode that differs from apoptosis, necrosis and autophagy, ferroptosis relies on iron and causes the buildup of intracellular lipid peroxides [12,13]. Generally, the induction of ferroptosis during the phases of ischemia and reperfusion may exacerbate myocardial ischemia—reperfusion injury [6]. At present, the protection provided by multiple biological and pharmacological inhibitions of ferroptosis protects the myocardium from IRI [14]. In addition, Slc7a11

* Correspondence to: Department of anesthesiology, the Affiliated Changzhou No 2 People's Hospital of Nanjing Medical University, Changzhou, China.
E-mail addresses: 490090270@qq.com (L. Zhu), wuzhouquan2005@126.com (Z. Wu).

¹ These authors contributed equally to this work.

² Present address: No. 68 Gehu Middle Road, Wujin District, Changzhou City, Jiangsu Province

and Gpx4, two of the most crucial targets whose inhibition elicits ferroptosis, are well regulated by Nrf2. The intention of the study is to determine the protective effect of ozone pretreatment on the myocardium during ischemia—reperfusion and the molecular mechanisms underlying its action.

2. Materials and methods

2.1. Reagents

Antibodies for Western blotting and immunostaining were obtained from the following sources: Anti-Nrf2 (WL02135) were purchased from Wanleibio (Shenyang, Liaoning, China); Anti-HO-1 (10701-1-AP), anti-GPX4 (67763-1-Ig) Proteintech Group (Wuhan, Hubei, China); Anti-GPX4 (CY6959), anti-Ferritin (CY5648), anti-xCT (CY7046) and DyLight 594-labeled goat anti-rabbit IgG (AB0151) were purchased from Abways (Shanghai, China); Horseradish peroxidase (HRP) Goat Anti-Rabbit IgG (AS014) and HRP Goat Anti-Mouse IgG (AS003) were purchased from Abclonal (Shanghai, China); DyLight 488-labeled goat anti-mouse IgG (AB0142) was purchased from ShareBio (Shanghai, China);

RNA used for transfection was obtained from the following resources: small interfering RNA for Nrf2 (siNrf2) and scrambled siRNA (siNC) were purchased from GenePharma (Shanghai, China); Lipofectamine RNAiMAX was purchased from Invitrogen (Shanghai, China).

Dyes: 2,3,5-triphenyltetrazolium chloride (TTC) and Evans blue dye were purchased from Sigma-Aldrich (America); 2', 7'-dichlorodihydrofluorescein diacetate (E004-1-1) (DCFH-DA) was purchased from Njjcbio (Nanjing, China); Mito-FerroGreen was purchased from Dojindo (Kumamoto, Japan).

Chemicals: DMEM (no glucose, serum nor sodium pyruvate) was purchased from Thermo Fisher Scientific (Shanghai, China); Erastin (HY-15763) and Fer-1 (HY-100579) were purchased from MedChemExpress (Beijing, China); Cell Counting Kit-8 (CCK-8) and BCA protein assay kit were purchased from Share-Bio (Shanghai, China); cytotoxicity detection kit, Total Superoxide Dismutase Assay Kit and lipid peroxide MDA detection kit were purchased from Beyotime (Shanghai, China).

2.2. Data acquisition and DEG screening

The GEO database was searched using (ischemia reperfusion) AND (myocardial), and the dataset was selected for the present analysis. The ferroptosis marker Ferrdb was searched. Dataset GSE153493 was based on the GPL19057 platform (Illumina NextSeq 500), which includes three normal samples and three ischemia reperfusion samples (<https://www.ncbi.nlm.nih.gov/geo/query/acc.cgi?acc=GSE153493>). Subsequently, differential gene expression (DEG) in normal samples and IR samples was analyzed based on linear model analysis of the microarray data package (LIMMA) in R software. At the same time, $|\log_{2}FC| > 2$ and P value < 0.05 were used as standard screening for the \log_{2} of the fold change ($\log_{2}FC$). The heatmap, volcano plot and Venn diagram were established with the application of the online tool Sangerbox (sangerbox.com). The “pheatmap” R package was used to construct the heatmap.

2.3. Function and transcription factor enrichment analysis of DEGs

Metascape is an online platform that not only provides various analysis tools for functional enrichment analysis and transcription factor prediction but also has the capability for annotating genes, searching for members and analyzing interactions between genes. To obtain the results of functional enrichment analysis and transcription factor analysis of differentially expressed genes (DEGs), we used Metascape in our study. To filter genes, we set three criteria: first, the P value of the screening results should be less than 0.01; second, the minimum count

should be 3; and finally, the enrichment factor should be greater than 1.5. Thus, we can determine that the results are statistically significant.

2.4. Protein—protein interaction (PPI) network analysis of mRNAs

To identify protein—protein interaction (PPI) networks of mRNA, an online search tool called the Search Tool for the Retrieval of Interacting Genes (STRING) database (<https://string-db.org>) was used for our analysis, with a filtering criterion set as a confidence score greater than 0.40 [15].

2.5. Animal model of ischemia/reperfusion (I/R) injury

Regarding the care and use of experimental animals, the National Institutes of Health in the United States has established guidelines (No. 85–23, revised 1996) that we have followed in our research involving experimental animals. Furthermore, the experimental protocol was approved by the Animal Research Committee, specifically the Animal Research Committee of Changzhou Second People's Hospital affiliated with Nanjing Medical University, which granted approval for the experiment. Acquired from and housed in the Changzhou Cavens Experimental Animals Co., Ltd., all of the adult male C57 mice aged 7 weeks (22–24 g) (4 per cage) were kept in an environment with controlled humidity and temperature and a 12-hour light and dark cycle. In accordance with the standards of humane care, water and food will be accessible to all mice, and a recovery period of 7 days prior to surgery will be provided.

The subjects of 36 mice in total were separated into 3 different groups by a random number table: (i) control (control, $n = 12$); (ii) control with IR surgery (I/R, $n = 12$); and (iii) IR plus ozone (25 $\mu\text{g}/\text{ml}$) pretreatment (I/R + O₃, $n = 12$). Prior to the surgery, for the control group, oxygen (2 ml on daily basis for 5 days) was intraperitoneally administered (i.p.); for the test group, an oxygen/ozone mixture (2 ml on a daily basis for 5 days) was administered (i.p.).

The method of ligating the left anterior descending coronary artery (LAD) creates an animal model [16]. Briefly, pentobarbital (50 mg/kg) was injected using a syringe and administered intraperitoneally to anesthetize the mice, while LAD establishment was performed using a 6–0 silk suture (Ningbo Medical Needle Co., Ltd., China). To test ST-T segment changes, electrocardiograms were subsequently monitored (FujifilmVisuaSonics, Toronto, ON, Canada). The ligature was released after 30 min of occlusion, and then the heart was subjected to 2 h reperfusion treatment. The same procedure should be implemented in the sham control group without ligating the LAD. In the closing period of reperfusion, we euthanized the mice by using sodium pentobarbital (100 mg/kg, ip) to harvest their hearts. Among the hearts, an Evans Blue-TTC assay was performed, 6 of which were utilized to measure the infarct size.

2.6. Determination of infarct size

As previously described, to assess myocardial infarct size, TTC was utilized [17]. Briefly, after reperfusion, the LAD was again occluded and stained with 3 ml of 1.5% Evans blue dye intravenously. Additional administration of sodium pentobarbital (100 mg/kg, i.p.) Following euthanasia of those mice as needed, the organs of the hearts were quickly harvested, the atria were abandoned, and the ventricles were cut into five uniform transverse slices using mouse heart matrix. Sections were fixed with 4% paraformaldehyde solution after incubation in 1% TTC for 20 min at 37 °C. By staining, we can clearly understand the size of myocardial infarction (IS) and the area at risk (AAR) of mouse hearts. The infarction area is shown as colorless, while the at-risk area is shown as red, and the nonischemic area is shown as blue. The collection and analysis of staining results were performed using a digital imaging system, which can assist us in better judging the heart condition of mice.

2.7. Cell culture and treatment

H9c2 cells were provided by the BeNa Culture Collection (Beijing Beina Chunglian Institute of Biotechnology) and cultured according to a previous description [16]. Meanwhile, cells at passages 3–9 were utilized.

An ozone-generating device (HUMARES GmbH, Shenyang, China) generates the ozone gas in need. The operating procedure was performed as previously described [18]. The medium was used to cultivate cells after being fully mixed with ozone, and these steps were performed before HR processing.

The H/R model was created as previously described [19], and PBS was used to rinse the cells twice. Then, the cells were cultured in DMEM without glucose, serum, or sodium pyruvate for 3 h in a hypoxia chamber containing 94% N₂, 5% CO₂ and 1% O₂, followed by reoxygenation for 3 h using complete high-glucose DMEM and 74% N₂, 5% CO₂ and 21% O₂.

The subsequent groups were tested: (1) Control group: the standard incubator became the place where the cells were preserved; (2) Erastin group: the cells were treated with 5 μM erastin at 37 °C for 3 h; (3) HR group: the cells were exposed to hypoxia and reoxygenation, each for 3 h; (4) HR+O₃ group: with pretreatment, the cells were placed in an ozone environment for 12 h before the HR treatment; (5) HR+O₃+Fer-1 group: the cells were treated with 10 μM Fer-1 at 37 °C for 2 h before the establishment of the model; (6) HR+O₃+Erastin group: the cells were treated with 5 μM erastin at 37 °C for 3 h prior to model establishment.

2.8. Cell viability and lactate dehydrogenase (LDH) release

With a CCK-8 assay, cell viability was measured in accordance with the manufacturer's directions. In short, 5×10^3 cells were inoculated into growth medium (100 μL) in a 96-well plate. In the closing period of treatment, CCK-8 solution (10 μL) was added to each well and incubated at 37 °C for 2 h. With a microplate absorbance reader (BioTek, USA), optical density (OD) values were determined at 450 nm. Meanwhile, what is expressed as a percentage of the control value is the index of cell viability.

Lactate dehydrogenase (LDH) was inspected with the application of a cytotoxicity detection kit complying with the kit manufacturer's instructions. Briefly, 5×10^3 cells were seeded in 96-well medium (100 μL), and LDH release solution (60 μL) was separately added to each well after treatment and incubated at 37 °C for 1 h. The level of LDH is demonstrated by measuring the optical density (OD) value at 490 nm (BioTek, USA), which is done utilizing a microplate reader, and the LDH level is expressed as a percentage of the control value.

2.9. Superoxide dismutase (SOD) and malondialdehyde (MDA) levels

Complying with the directions from the manufacturer, the intracellular SOD activities were measured using a Total Superoxide Dismutase assay kit. In brief, 1×10^6 cells were seeded in a 6 cm plate. In the closing period of treatment, cells were harvested, SOD sample preparation solution and centrifuged at 12,000g for 5 min. The WST-8/enzyme working solution was reacted with the supernatants, and the reaction products were spectrophotometrically evaluated in a gauge at 450 nm and the products after the reaction were measured spectrophotometrically at 532 nm (BioTek, USA). SOD activity is regarded as a percent of the control value.

With the requirements of the instructions for use of the lipid peroxide MDA detection kit, intracellular MDA levels were measured accordingly. Briefly, after seeding in 6-cm plates, the 1×10^6 cells in use were grown to the appropriate density. They were then lysed with cell lysate for 10 min and collected, the supernatant after cryocentrifugation reacted with thiobarbituric acid (TBA), and the products after the reaction were measured spectrophotometrically at 532 nm (BioTek, USA). The entire experiment was repeated in triplicate, where nmol/mg protein was used

to represent the level of MDA.

2.10. Reactive oxygen species (ROS) determination

For detection of reactive oxygen species, an ROS fluorescence probe (DCFH-DA, E004-1-1) was utilized as instructed by the manufacturer's protocol. Plated on 6-well plates, H9c2 cells were incubated with 10 μmol/L DCFH-DA (diluted in serum-free DMEM) at 37 °C for 30 min in darkness after treatment. With serum-free DMEM, the cells were washed twice and then collected for flow cytometry.

2.11. Detection of mitochondrial labile iron

With the help of the manufacturer's protocol, aiming at detecting mitochondrial labile iron, the fluorophore Mito-FerroGreen was utilized accordingly. H9c2 cells were plated on 14 mm round cell slides in 24-well plates and incubated with 5 μmol/L FerroGreen (diluted in DMEM without serum) at 37 °C for 30 min in lightless surroundings after treatment. By using serum-free DMEM, the cells were washed twice. Fluorescence was visualized with the support of a fluorescence microscope (Nikon A1R, Shanghai, China).

2.12. Immunofluorescence assay detecting Nrf2-Gpx4 coexpression and Nrf2 nuclear translocation

To understand the coexpression of Nrf2-Gpx4 and nuclear translocation of Nrf2, immunofluorescence staining was performed. Round cell slides (14 mm) were placed in a 24-well cell culture plate after sterilization, and H9c2 cells were seeded in the plate for cell adhesion. After the cells adhered to the slide, they were subjected to corresponding treatments and then fixed with 4% paraformaldehyde after treatment. After removing the cell slide, 5% goat serum was added and incubated at room temperature for 1 h, followed by washing with PBS. Nrf2 (1:50) and Gpx4 (CY6959, 1:50) antibodies were added to the cell slide and incubated overnight at 4 °C. After primary antibody incubation, excess primary antibody was removed with PBS. Goat anti-mouse IgG (DyLight 488, 1:50) and goat anti-rabbit IgG (DyLight 594, 1:50) were added and incubated at 37 °C for 1 h. The excess secondary antibody was washed with PBS, and DAPI was added to stain the cell nucleus. The results were observed with a fluorescence microscope.

2.13. Western blotting

As previously described, followed by western blot analysis, the processed cardiomyocytes were collected and digested. A BCA protein assay kit was used to determine the protein concentration. Using 15% SDS-PAGE gels, samples of protein were separated by electrophoresis. Soon afterward, they were transferred to nitrocellulose (NC) filter membranes from Millipore. The cell membranes were incubated with the corresponding primary antibodies (Nrf2, HO-1, GPX4 (67763-1-Ig), Ferritin and xCT, 1:1000) at 4 °C for one night. Then, the membrane was incubated with horseradish peroxidase (HRP) goat anti-rabbit IgG (AS014) or HRP goat anti-mouse IgG (AS003) secondary antibody 1:4000 at room temperature for 1 h. In succession, the membranes were washed three times in TBST. With the utilization of ProteinSimple FluorChemQ2 and ImageJ software 1.53 (National Institutes of Health), digital images of immunoblots were attained, and the densitometry of the bands was analyzed.

2.14. SiRNA transfection

Prior to transfection, H9c2 cells were seeded in 6-well plates overnight. Transfection was carried out using siNrf2 (50 nM) and siNC with the assistance of Lipofectamine RNAiMAX following the manufacturer's protocol. Cells treated with or without HR at the indicated times after 36 h of incubation were collected. This method appears in three different

uses described previously: western blotting, flow cytometry assay, and tolerant immunofluorescence assay.

2.15. Statistical analysis

Analysis of all data was obtained based on the statistical software GraphPad Prism (version 5.0). Confirmation of normal distribution was obtained based on the Shapiro–Wilk test ($P > 0.1$) for SPSS (version 17.0). With the application of one-way ANOVA, the disparity between each group was analyzed. $P < 0.05$ was judged statistically significant. To confirm where the disparities emerged between groups. Further Tukey post hoc analysis ($\alpha = 0.05$) was accomplished.

3. Results

3.1. In ischemia–reperfusion-triggered cardiac impairment, ferroptosis is of extreme significance

GEO2R is software that can analyze DEGs in transcriptome gene datasets online, which we used to identify DEGs in the GSE153493 dataset associated with a myocardial I/R rat model. To set the cutoff criteria, we applied p value < 0.05 and $|\log_{2}FC| > 2$. The GSE153493 dataset includes an IR group and a sham group. To demonstrate the DEGs obtained through analysis by GEO2R, we used volcano plots and heatmaps for illustration. (Fig. 1 A and B). The results of volcano plots

and heatmaps showed that the expressions of ferroptosis related regulatory factors Slc7a11 [20], Hmox1 [21] and Ptgs2 [22] in I/R are significantly increased, pointing to the likely involvement of ferroptosis in pathology during myocardial I/R. The Venn diagram shows the intersecting genes of DEGs of GSE153493 and markers of the Ferrdb database, including 31 common genes with altered expression: Slc7a11, Hmox1, Ptgs2, etc. (Fig. 1 C). To demonstrate that ischemia–reperfusion injuries might provoke cellular ferroptosis, H9c2 cells were pretreated with the ferroptosis inhibitor Fer-1 and then subjected to H/R. Our analysis revealed that, compared with the H/R Model group, Fer-1 pretreatment resulted in an evident increase in cell viability (H/R+ Fer-1 group vs. H/R Model group, 0.819 ± 0.03 vs. 0.532 ± 0.02 , $P < 0.001$, Fig. 1 D) and significantly reduced LDH release (H/R+ Fer-1 group vs. H/R Model group, 1.00 ± 0.02 vs. 2.12 ± 0.27 , $P < 0.001$, Fig. 1 E). Our research has similar results to those of previous studies [6, 23], which indicates that the development of MIRI is closely related to ferroptosis and may play a decisive role in the pathological progression of MIRI.

3.2. Regarding the regulation of myocardial I/R injury, Nrf2 (Nfe2l2) is one of the most essential transcription factors

To investigate the mechanism of MIRI-induced ferroptosis, further efforts were made to perform GO and KEGG enrichment analyses in view of these 31 DEGs. Interestingly, as one of the biological processes that

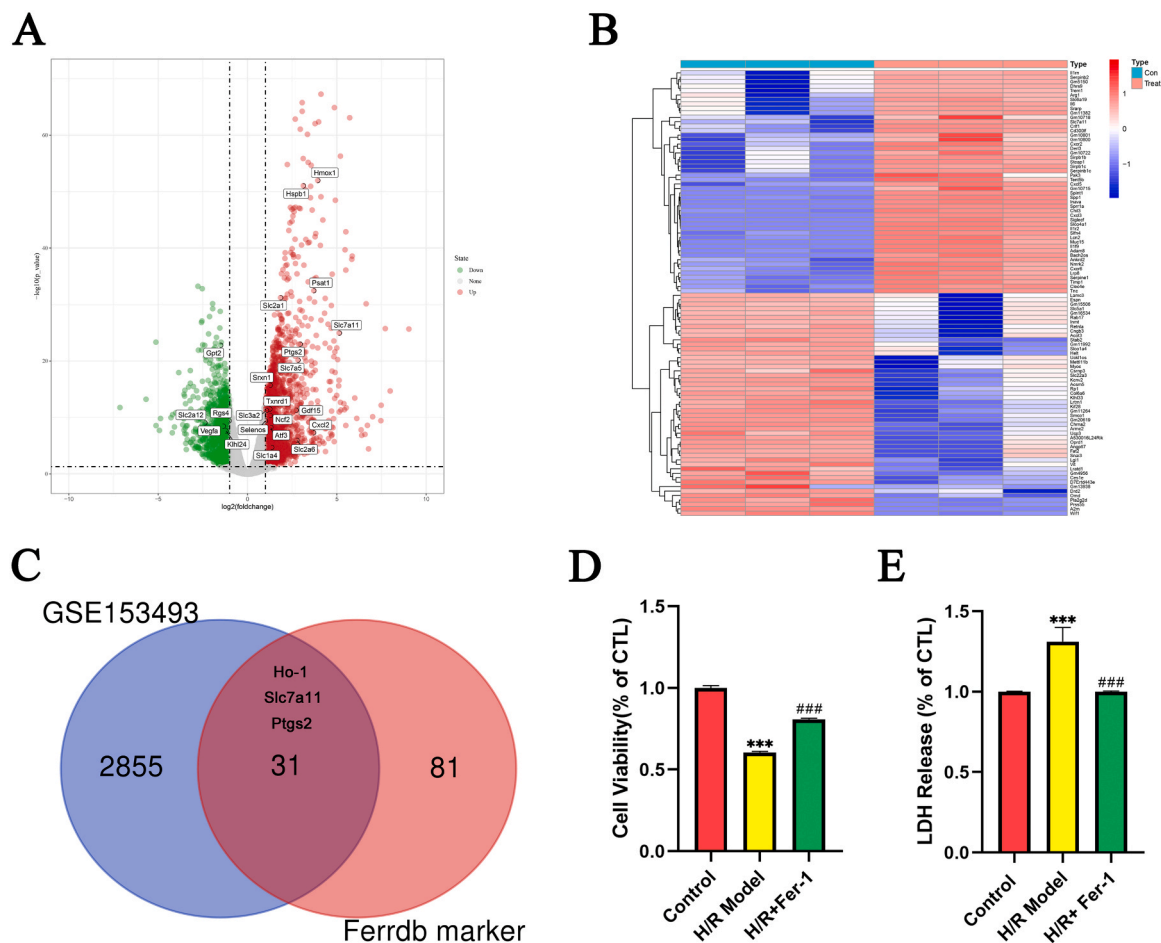


Fig. 1. In the ischemia reperfusion induced cardiac impairment, the role of ferroptosis is vital. (A) What the volcano plot displays is the distribution of DEGs of the GSE153493 datasets. (B) The up-regulated and down-regulated DEGs extracted from the GSE153493 datasets, whose expression level was demonstrated by the heatmap. (C) The Venn diagram presents the common DEGs in the GSE153493 datasets and Ferrdb Marker. (D) Cell viability was analyzed by CCK8 assay in the H9c2 cardiomyocytes after HR injury with or without Fer-1 pre-treatment. (E) LDH release in the H9c2 cardiomyocytes after HR injury with or without Fer-1 pre-treatment. All experiments were repeated three times. The data were represented as the means \pm SEM. *** $P < 0.001$ vs. Control; ### $P < 0.001$ vs. H/R Model.

was affected most by MIRI, the response to oxidative stress was suggested to play a significant role (Fig. 2 A and B). We also performed transcription factor enrichment analysis based on these 31 DEGs. Among them, nuclear factor erythrocyte-like 2 (Nrf2, also known as Nfe2l2) ranks high, so it is speculated that Nrf2 may play a significant role as one of the most important transcription factor responses to oxidative stress (Fig. 2 C). The PPI networks of these 31 DEGs were generated based on the STRING database. Based on the strongest interactions among genes, we selected two hub genes: Ho-1 and Slc7a11 (Fig. 2 D and E).

3.3. Ozone could alleviate I/R-induced cardiac impairment

As shown in vivo, the mechanism by which ozone prevents I/R injury is to reduce cardiac risk (I/R+O3 group vs. I/R group 1050.51 ± 14.99 vs. 1935.34 ± 79.97 , $P < 0.001$, Fig. 3 A) and infarct size as well as to reduce ST elevation (I/R+O3 group vs. I/R group, 1511.48 ± 101.96 vs. 1805.38 ± 94.96 , $P = 0.0172$, Fig. 3 B). To elaborate on the protective concentration of ozone from the perspective of cardiomyocytes, different doses of ozone were used to treat H9c2 cells. Our study showed that incubation with 20 $\mu\text{g/ml}$ ozone for 24 h had no significant toxicity to H9c2 cells (0.99 ± 0.02 , Fig. 3 C). Similarly, to assess the protective effect of ozone against H/R-induced cardiomyocyte injury, we pretreated H9c2 cells with ozone at concentrations of 10–60 $\mu\text{g/ml}$. As

shown in Fig. 3 D, the cell viability was significantly improved after pretreatment of H9c2 cells with different concentrations of ozone, and the best effect was obtained at a concentration of 20 $\mu\text{g/ml}$ (0.88 ± 0.04).

3.4. Ozone pretreatment exerts a protective effect on H9c2 cells by inhibiting ferroptosis and enhancing the antioxidant capacity

Since ozone pretreatment at 20 $\mu\text{g/ml}$ had the best protective effect on H9c2 cells (Fig. 3 D), the component alteration of ferroptosis was explored in the next step by western blot assay. As shown in Fig. 4 A and G, compared with controls, the expression of Nrf2 (Control vs. H/R group, 0.29 ± 0.01 vs. 0.72 ± 0.01 , $P < 0.001$; Control vs. Erastin group, 0.29 ± 0.01 vs. 0.52 ± 0.02 , $P < 0.001$), Gpx4 (Control vs. H/R group, 0.48 ± 0.01 vs. 0.77 ± 0.01 , $P < 0.001$; Control vs. Erastin group, 0.48 ± 0.01 vs. 0.65 ± 0.03 , $P < 0.001$) and Fth-1 (Control vs. H/R group, 0.43 ± 0.02 vs. 0.70 ± 0.05 , $P < 0.001$; Control vs. Erastin group 0.43 ± 0.02 vs. 0.63 ± 0.01 , $P < 0.001$) and the activity of SOD (Control vs. H/R group, 1.00 ± 0.02 vs. 1.79 ± 0.04 , $P < 0.001$; Control vs. Erastin group, 1.00 ± 0.02 vs. 1.92 ± 0.08 , $P < 0.001$) were slightly upregulated after H/R and erastin treatment but significantly upregulated after ozone pretreatment (Control vs. H/R+O3 group, Nrf2, 0.29 ± 0.01 vs. 1.15 ± 0.024 , $P < 0.001$; Gpx4, 0.48 ± 0.01 vs. 1.09 ± 0.04 ,

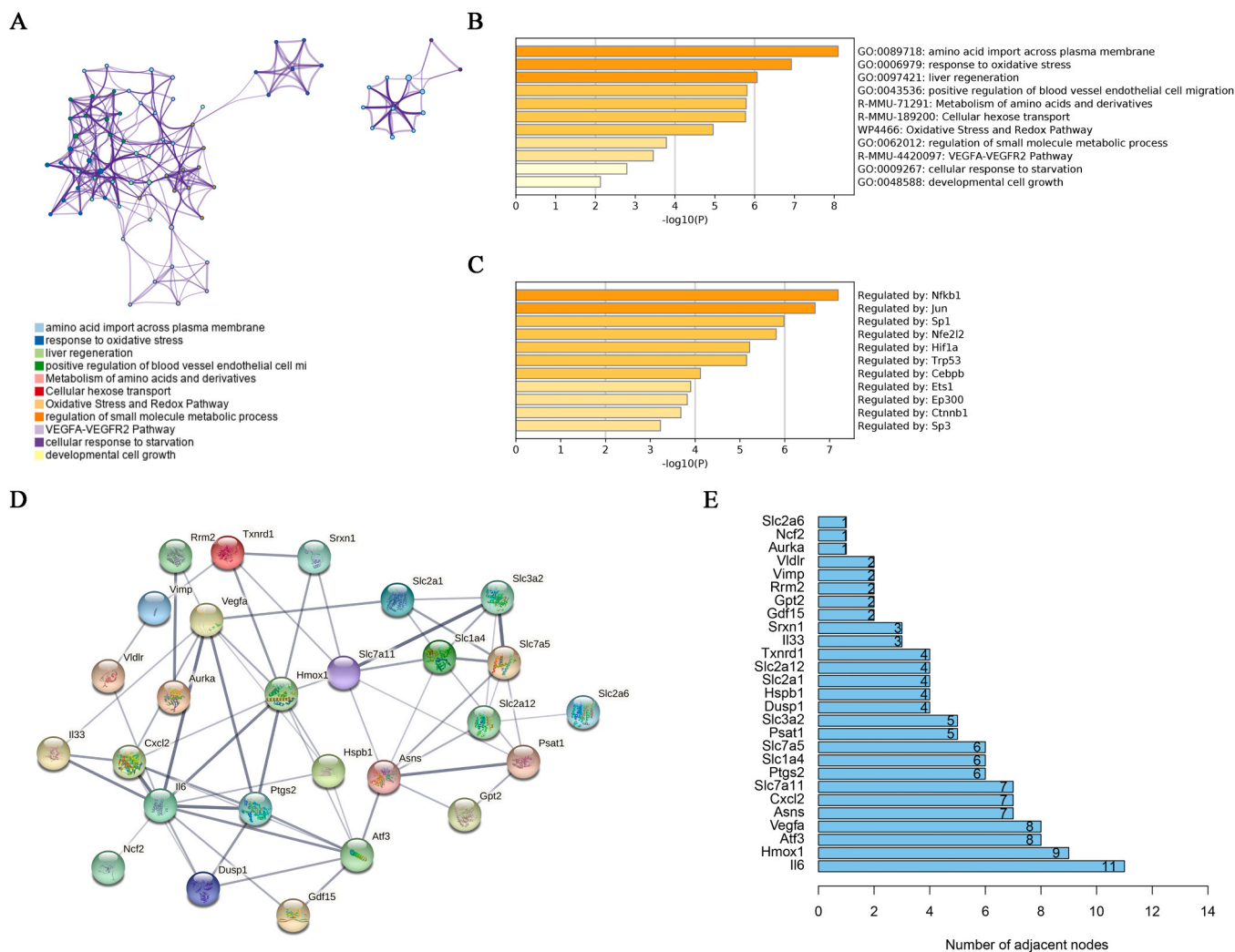


Fig. 2. : Nrf2 (Nfe2l2) is an important transcription factor regulating myocardial ischemia-reperfusion injury. (A)The function and connection enriched terms colored by clusters are presented by the network. (B) The column diagram shows the GO functional and KEGG pathway enrichment analysis of 31 DEGs. (C) Above column diagram shows the transcription factor enrichment analysis of 31 DEGs. (D) The network presents the protein-protein interactions of 31 DEGs. (E) The column diagram shows the number of adjacent nodes based on the PPI network.

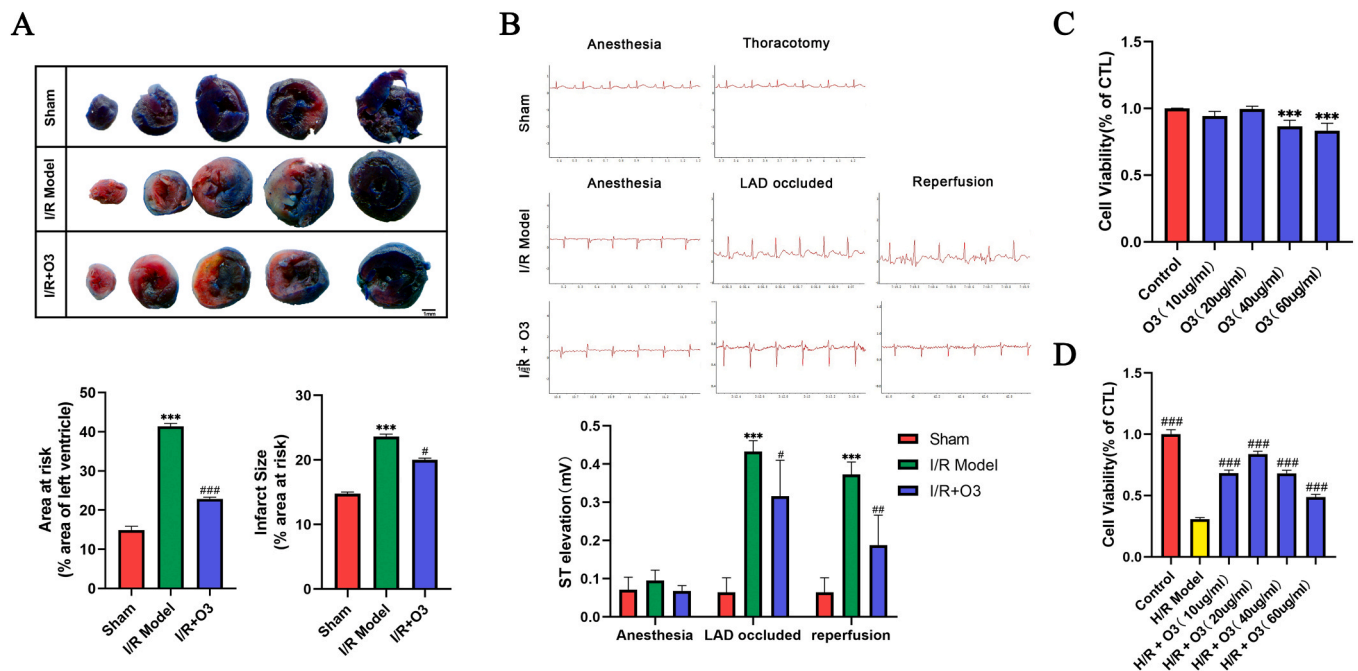


Fig. 3. : Ozone alleviate ischemia reperfusion induced cardiac impairment. (A) Evans blue-TTC double staining measures the Area at risk and Infarct size in the representative images and analysis results. Scale bar = 1 mm; (B) ECG monitoring was used for the representative images and analysis results of ST segment elevation. All experiments were repeated three times. *** $P < 0.001$ vs. Sham; # $P < 0.05$, ## $P < 0.01$, and ### $P < 0.001$ vs. I/R Model. (C and D) Ozone treatment on cell viability in H9c2 cardiomyocytes with or without H/R injury. All experiments were repeated three times. The data were represented as the means \pm SEM. * $P < 0.05$ vs. Control; # $P < 0.05$, ## $P < 0.01$, and ### $P < 0.001$ vs. H/R Model.

$P < 0.001$; Fth-1, 0.43 ± 0.02 vs. 0.92 ± 0.01 , $P < 0.001$; SOD, 1.00 ± 0.02 vs. 2.46 ± 0.088 ; $P < 0.001$). Interestingly, we found in H/R and erastin treatment that Ho-1 (Control vs. H/R group, 0.51 ± 0.03 vs. 0.87 ± 0.06 , $P < 0.001$; Control vs. Erastin group, 0.51 ± 0.03 vs. 0.70 ± 0.02 , $P < 0.001$) and Slc7a11 (Control vs. H/R group, 0.44 ± 0.03 vs. 0.32 ± 0.02 , $P < 0.001$; Control vs. Erastin group, 0.44 ± 0.03 vs. 0.63 ± 0.01 , $P < 0.001$) express themselves differently, which was significantly upregulated by ozone pretreatment (Ho-1, Control vs. H/R+O3 group, 0.51 ± 0.03 vs. 1.15 ± 0.03 , $P < 0.001$; Slc7a11, Control vs. H/R+O3 group, 0.44 ± 0.03 vs. 1.11 ± 0.04 ; $P < 0.001$). Furthermore, we explored the coexpression of Nrf2 and Gpx4 and Nrf2 nuclear translocation by immunofluorescence staining (Fig. 4 B). The coexpression of Nrf2 and Gpx4 as well as the degree of nuclear translocation of Nrf2 rose slightly after HR and erastin treatment, while the expression was more pronounced after ozone pretreatment. The levels of ROS were detected with the assistance of flow cytometry, and the results indicated that H/R and erastin treatment significantly upregulated ROS levels, while ozone pretreatment partially reversed this effect (Fig. 4 C). Similar to the change in ROS levels, H/R and erastin treatment significantly increased the level of mitochondrial iron (Fig. 4 D), MDA (Control vs. H/R+O3 group, 1.00 ± 0.04 vs. 2.40 ± 0.27 , $P < 0.001$, Fig. 4 H) and LDH (Control vs. H/R+O3 group, 1.00 ± 0.02 vs. 1.06 ± 0.08 , $P < 0.001$, Fig. 4 F) release, which was partially rescued by ozone pretreatment. Collectively, these data suggest that H/R (Control vs. H/R group, 1.00 ± 0.06 vs. 0.56 ± 0.02 , $P < 0.001$, Fig. 4 E) and erastin (Control vs. Erastin group, 1.00 ± 0.06 vs. 0.55 ± 0.01 , $P < 0.001$, Fig. 4 E) treatment dramatically decreased cell viability, which was rescued by ozone pretreatment (Control vs. H/R+O3 group, 1.00 ± 0.06 vs. 0.88 ± 0.03 , $P < 0.001$, Fig. 4 E).

3.5. The protective effect of ozone pretreatment was enhanced by Fer-1 and inhibited by erastin

To demonstrate the vital effect of ferroptosis on MIRI, we introduced Fer-1 and erastin treatment on the basis of ozone pretreatment. As

shown in Fig. 5 A and G, the results after using a ferroptosis inhibitor denoted that the expression of Nrf2 (H/R+O3 group vs. H/R+O3 + Fer-1 group, 0.71 ± 0.01 vs. 0.99 ± 0.02 , $P < 0.001$), Ho-1 (H/R+O3 group vs. H/R+O3 + Fer-1 group, 0.70 ± 0.03 vs. 0.94 ± 0.04 , $P < 0.001$), Slc7a11 (H/R+O3 group vs. H/R+O3 + Fer-1 group, 0.87 ± 0.02 vs. 1.14 ± 0.02 , $P < 0.001$), Gpx4 (H/R+O3 group vs. H/R+O3 + Fer-1 group, 0.89 ± 0.01 vs. 1.05 ± 0.03 , $P < 0.001$) and Fth-1 (H/R+O3 group vs. H/R+O3 + Fer-1 group, 0.74 ± 0.01 vs. 0.93 ± 0.02 , $P < 0.001$) and the activity of SOD (H/R+O3 group vs. H/R+O3 + Fer-1 group, 1.65 ± 0.07 vs. 2.34 ± 0.11 , $P < 0.001$) were significantly upregulated in the Fer-1 group in contrast with the ozone pretreatment group. Interestingly, these upregulated proteins were downregulated in the erastin group (H/R+O3 + Fer-1 group vs. H/R+O3 + Erastin group, Nrf2, 0.99 ± 0.02 vs. 0.72 ± 0.024 , $P < 0.001$; Ho-1, 0.94 ± 0.04 vs. 0.55 ± 0.04 , $P < 0.001$; Slc7a11, 1.14 ± 0.02 vs. 0.58 ± 0.02 , $P < 0.001$; Gpx4, 1.05 ± 0.03 vs. 0.47 ± 0.02 ; $P < 0.001$; Fth-1, 0.93 ± 0.02 vs. 0.36 ± 0.03 , $P < 0.001$). The next section of the study was concerned with the coexpression of Nrf2 and Gpx4 and Nrf2 nuclear translocation. In comparison to the ozone pretreatment group, the coexpression of Nrf2 and Gpx4 as well as Nrf2 nuclear translocation were significantly upregulated in the Fer-1 group and downregulated in the erastin group (Fig. 5 B). Turning now to the experimental evidence on the level of ROS, Fer-1 treatment further reduced the level of ROS on the basis of ozone pretreatment but was reversed by erastin treatment (Fig. 5 C). Similar to the change in ROS levels, compared with ozone treatment, Fer-1 treatment further decreased the levels of mitochondrial iron (Fig. 5 D), MDA (H/R+O3 + Fer-1 group vs. H/R+O3 + Erastin group, 0.57 ± 0.04 vs. 1.57 ± 0.27 , $P < 0.001$, Fig. 5 H) and LDH (H/R+O3 + Fer-1 group vs. H/R+O3 + Erastin group, 0.49 ± 0.12 vs. 1.35 ± 0.26 , $P < 0.001$, Fig. 5 F) release, but these effects were reversed by erastin treatment. In summary, these results show that the protective effect of ozone pretreatment could be enhanced although Fer-1 treatment but reversed by erastin treatment (H/R+O3 + Fer-1 group vs. H/R+O3 + Erastin group, 1.86 ± 0.78 vs. 0.73 ± 0.13 , $P < 0.001$, Fig. 5 E).

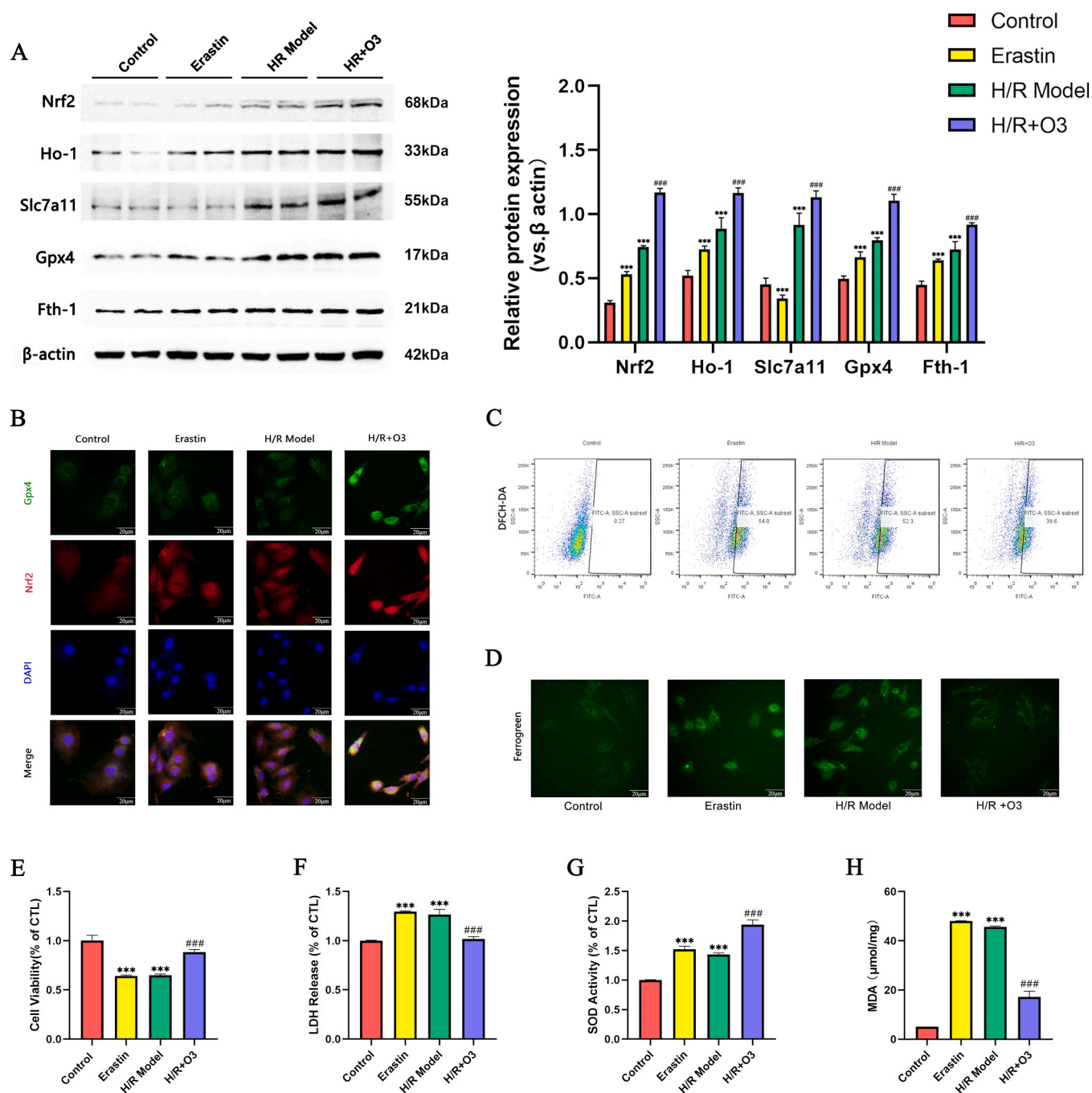


Fig. 4. : Ozone pretreatment exerts a protective effect by inhibiting the ferroptosis and enhance the anti-oxidative of H9c2 cells. (A)The effect of Ozone pretreatment on the expression of Nrf2, Ho-1, Slc7a11, Gpx4 and Fth-1 in H9c2 cardiomyocytes after H/R injury. (B) Representative immunofluorescence images of Nrf2 (red) and Gpx4 (green) co-expression and the Nrf2 nuclear translocation in H9c2 cardiomyocytes after HR injury with or without Ozone pretreatment. (C and D) Representative images of ROS production and mitochondrial ferrous ions aggregation in H9c2 cardiomyocytes after HR injury with or without Ozone pretreatment. (E-G) Effects of Ozone pretreatment on Cell viability, LDH release, SOD activity and MDA production in H9c2 cardiomyocytes after HR injury. All experiments were repeated three times. The data were represented as the means \pm SEM. *** $P < 0.001$ vs. Control; ### $P < 0.001$ vs. H/R Model.

3.6. The protective effect of ozone pretreatment on H9c2 could be counteracted after the Nrf2 gene was knocked down

We used Nrf2-siRNA to transfect H9c2 cells to complementarily validate the involvement of the Nrf2/Slc7a11/Gpx4 axis in the protective effect of ozone pretreatment. Induced by ozone pretreatment in H/R, the protein expression of Nrf2, Ho-1, Slc7a11, Gpx4 and Fth-1 and the activity of SOD were dramatically reduced in Nrf2-knockdown cells (H/R+O3 group vs. H/R+O3 +siNrf2 group, Nrf2, 0.52 ± 0.01 vs. 0.17 ± 0.01 , $P < 0.001$; Ho-1, 0.72 ± 0.03 vs. 0.46 ± 0.02 , $P < 0.001$;

Slc7a11, 0.93 ± 0.01 vs. 0.40 ± 0.04 , $P < 0.001$; Gpx4, 0.96 ± 0.07 vs. 0.41 ± 0.04 ; $P < 0.001$; Fth-1, 1.08 ± 0.04 vs. 0.63 ± 0.04 , $P < 0.001$; SOD, 1.40 ± 0.59 vs. 0.62 ± 0.03 ; $P < 0.001$; Fig. 6 A and G). Regarding the coexpression of Nrf2 and Gpx4 and Nrf2 nuclear translocation, Nrf2 knockdown abolished these effects of ozone pretreatment (Fig. 6 B). Nrf2 knockdown abrogated both the reduction in ROS (Fig. 6 C) and MDA levels (H/R+O3 group vs. H/R+O3 +siNrf2 group, 0.61 ± 0.02 vs. 1.50 ± 0.01 , $P < 0.001$, Fig. 6 H), the level of mitochondrial iron (Fig. 6 D) and the release of LDH (H/R+O3 group vs. H/R+O3 +siNrf2 group, 0.70 ± 0.02 vs. 1.07 ± 0.06 , $P < 0.001$, Fig. 6 C). Overall, these results

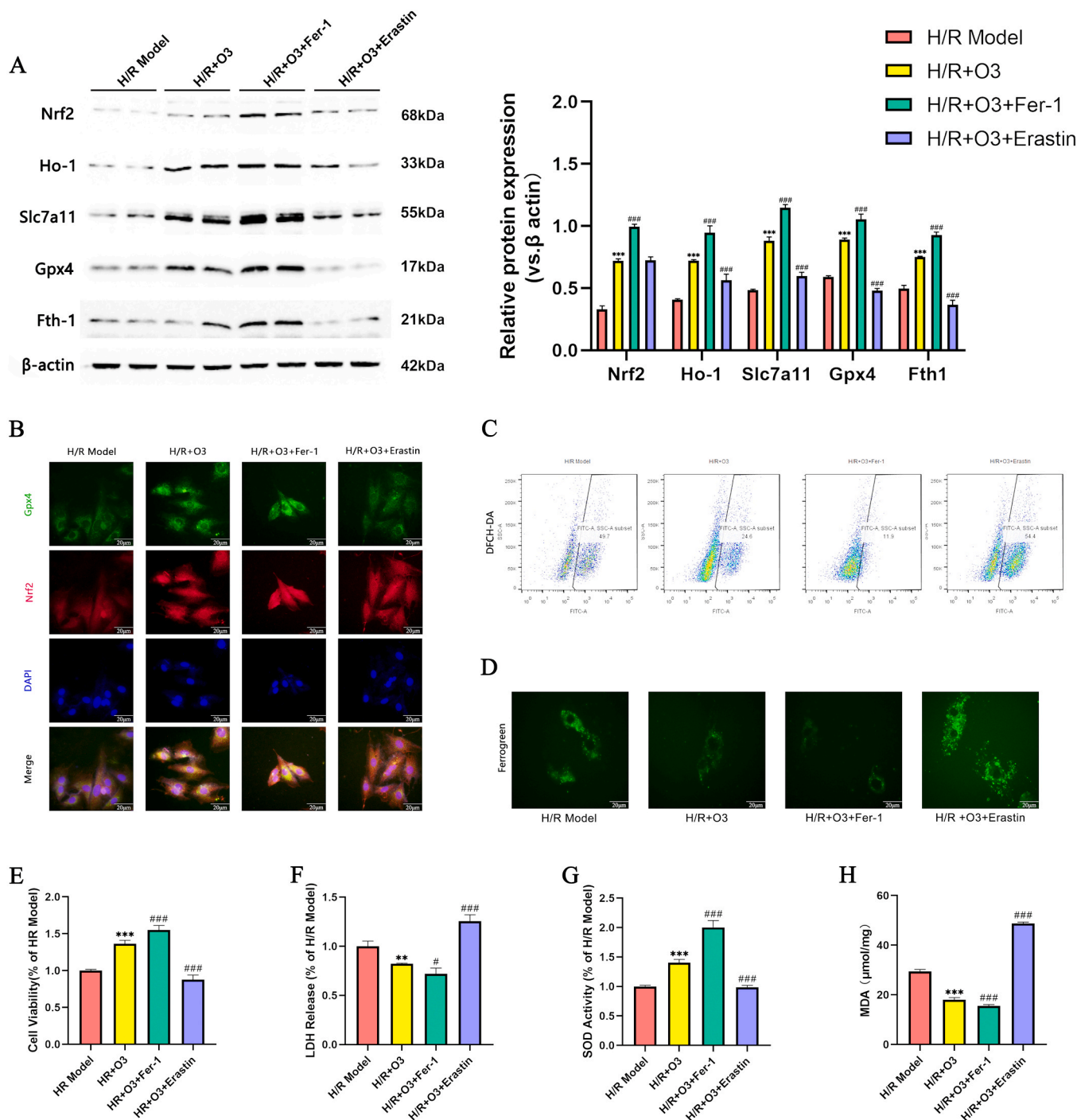


Fig. 5. : The protective effect of ozone pretreatment was enhanced by Fer-1 and inhibited by Erastin. (A)The protein expression of Nrf2, Ho-1, Slc7a11, Gpx4 and Fth-1 in the H9c2 cardiomyocytes after HR injury with Ozone pretreatment in the presence of Fer-1 or Erastin. (B) Representative immunofluorescence images of Nrf2 (red) and Gpx4 (green) co-expression and the Nrf2 nuclear translocation in the H9c2 cardiomyocytes after HR injury with Ozone pretreatment with Fer-1 or Erastin. (C and D) Representative images of ROS production and mitochondrial ferrous ions aggregation in the H9c2 cardiomyocytes after HR injury with Ozone pretreatment with Fer-1 or Erastin. (E-G) Effects of Ozone production on Cell viability, LDH release, SOD activity and MDA production in the H9c2 cardiomyocytes after HR injury with Ozone pretreatment with Fer-1 or Erastin. All experiments were repeated three times. The data were represented as the means \pm SEM. * * $P < 0.01$, and * * * $P < 0.001$ vs. H/R Model; # $P < 0.05$, and ### $P < 0.001$ vs. H/R+O3 group.

indicate that Nrf2 knockdown abolishes the protective effects of ozone pretreatment (H/R+O3 group vs. H/R+O3 +siNrf2 group, 1.53 ± 0.05 vs. 0.99 ± 0.04 , $P < 0.001$, Fig. 6 E).

4. Discussion

This research demonstrated that ozone pretreatment is

cardioprotective against I/R injury by at least partially enhancing the antioxidant stress capacity and reducing ferroptosis in H9c2 cells. Both in vivo and in vitro experiments provide evidence that ozone pretreatment can reduce myocardial I/R injury, especially in vitro experiments, further confirming that regulating the expression of iron-related proteins and promoting Nrf2 nuclear translocation are the ways in which ozone pretreatment exerts protective effects. Based on the above

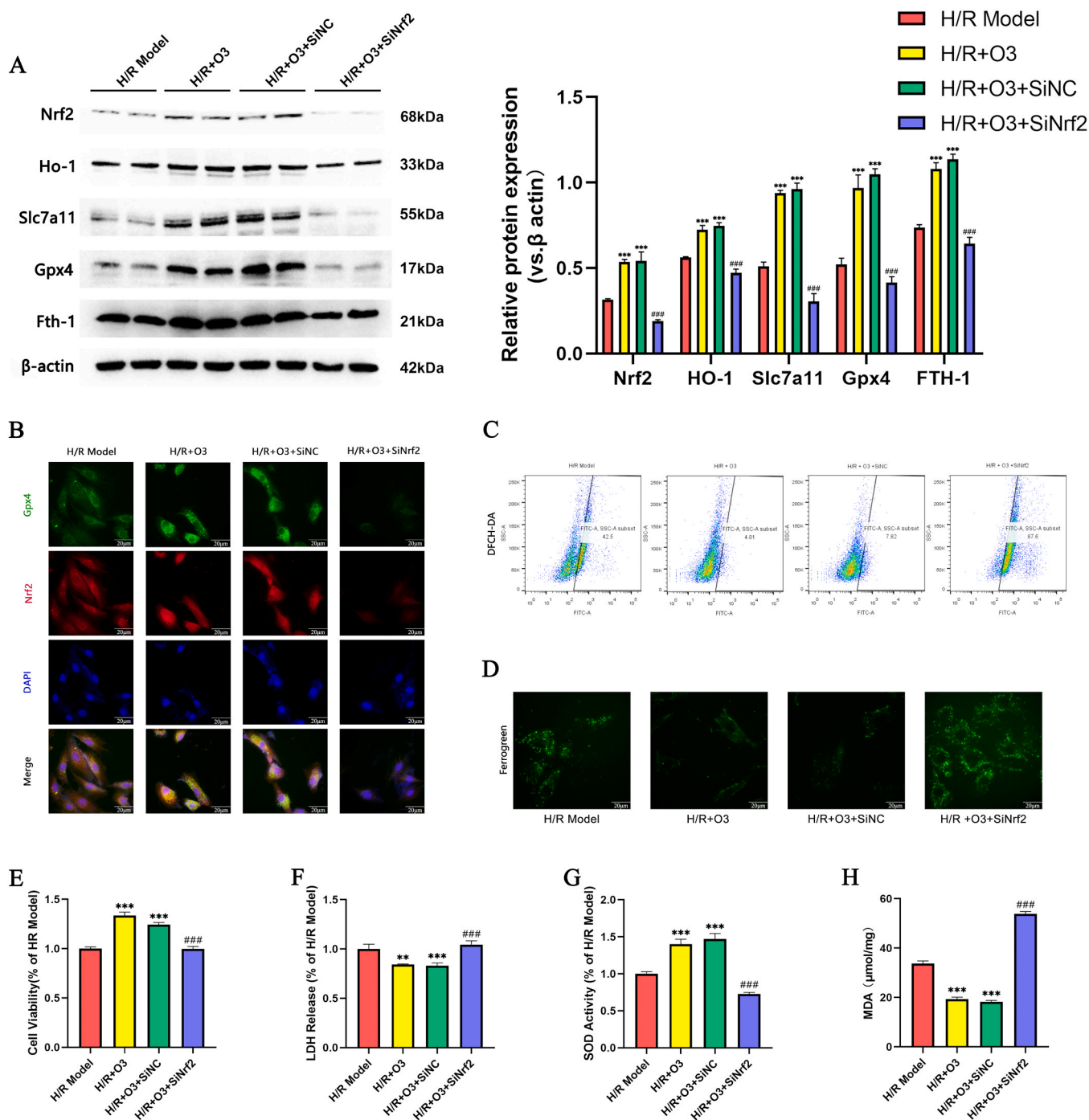


Fig. 6. Genetic knockdown of Nrf2 abrogates the protective effect of Ozone pretreatment on H9C2 cell. (A) The protein expression of Nrf2, Ho-1, Slc7a11, Gpx4 and Fth-1 in the company of siNrf2 or siNC with or without Ozone pretreatment in H9c2 cells after HR treatment. (B) Representative immunofluorescence images of Nrf2 (red) and Gpx4 (green) co-expression and the Nrf2 nuclear translocation in the company of siNrf2 or siNC with or without Ozone pretreatment in H9c2 cells after HR treatment. (C and D) Representative images of ROS production and mitochondrial ferrous ions aggregation in the company of siNrf2 or siNC with or without Ozone pretreatment in H9c2 cells after HR treatment. (E-G) Effects of Ozone production on Cell viability, LDH release, SOD activity and MDA production in the company of siNrf2 or siNC with or without Ozone pretreatment in H9c2 cells after HR treatment. All experiments were repeated three times. The data were represented as the means \pm SEM. * $P < 0.01$, and ** $P < 0.001$ vs. H/R Model; ### $P < 0.001$ vs. H/R+O3 +SiNC group.

research, we have concluded that the protective effect of ozone in alleviating myocardial I/R injury is at least accomplished through the Nrf2/Slc7a11/Gpx4 axis, which may offer innovative approaches and a materialization of ozone as a prospective treatment for ischemic heart disease.

During reperfusion, excessive release of ROS is due to an imbalance in iron homeostasis, resulting in a rise in free iron undergoing a Fenton

reaction [24]. Subsequently, the exacerbation of ROS production produces damage by oxidizing proteins, DNA and lipids [25]. As a result, cytochrome release and calcium overload benefit from increased mitochondrial outer membrane permeability and can trigger downstream cell death mechanisms [26,27]. Consistently, our study obtained 31 DEGs from the intersection of dataset GSE0153493 and Ferrdb marker (Fig. 1), and pathway enrichment analysis of DEGs implied that

these genes were primarily related to the response to oxidative stress and regulated by Nrf2 (Fig. 2). Ozone can stimulate the activation of antioxidant enzymes such as CAT, HO-1, quinone oxidoreductase 1 (NQO1), and SOD [28]. As a previous study showed, ozone was able to exert a conserving effect during myocardial injury by enhancing antioxidant effects and reducing mitochondrial damage [10].

As one of the most potent oxidizers, low concentrations of ozone can induce an antioxidant response to reverse oxidative stress [29]. An increasing number of prior experiments have noted the biomedical effects of ozone-assisted therapy in pain management [30], gastrointestinal diseases [31], lung diseases [32], diabetes [33], ischemia injury [34], cancer [35], infective diseases [36], dentistry [37], etc. For example, Meng et al. confirmed that ozone can reduce myocardial ischemia—reperfusion injury by activating the Nrf2/Are pathway, and the role of ozone in myocardial ischemic diseases needs to be further explored and studied in depth. Our study first argued that the protective effect of ozone pretreatment might be associated with attenuated ferroptosis. The *in vivo* study confirmed that ozone pretreatment reduced the risk and infarct area and decreased ST elevation (Fig. 3 A and Fig. 3 B), and the *in vitro* study confirmed that ozone pretreatment reduced the release of LDH and improved cell viability (Fig. 3 C and Fig. 3 D), which suggests the capability of ozone to mitigate myocardial IR injury.

The reaction of ozone with water-soluble antioxidants, such as polyunsaturated fatty acids (PUFAs), could create products that are capable of mediating ozone-induced biochemical effects [29]. After mixing with blood, ozone interacts with substances such as PUFAs [38]. During this process, generated hydrogen peroxide and lipid oxidation products serve as signaling molecules, playing a positive role in regulating the effects of biochemical processes. Bell et al. suggested that mild oxidative stress could upregulate Nrf2 expression in astrocytes under subtoxic levels of hydrogen peroxide stimulation, thus exerting a neuroprotective role in ischemic preconditioning [14]. This is consistent with our findings that the use of ozone during the myocardial ischemia—reperfusion injury process can reduce the degree of damage while enhancing myocardial protection. Ozone may regulate the expression of Nrf2, thereby improving oxidative stress pathways to exert antioxidant capacity.

In addition, our study also found that ozone was able to inhibit ferroptosis by activating the upstream Nrf2/Slc7a11/Gpx4 signaling pathway (Fig. 4). Thus, ferroptosis inducers and inhibitors were applied to investigate the protective effect of ferroptosis modulation by ozone pretreatment. Erastin, an Slc7a11 inhibitor, has been reported to cause ferroptosis by inducing ROS production and free iron augmentation [39]. Consistently, the *in vitro* study showed that erastin induced ROS exacerbation and mitochondrial iron assembly under H/R and overrode the protective effect of ozone against ferroptosis (Fig. 5 C and D). Fer-1, an Slc7a11 inducer, was reported to suppress ferroptosis by decreasing the production of ROS and augmenting free iron [40]. Coincidentally, our study showed that Fer-1 enhanced the protective effect of ozone pretreatment by reducing ROS exacerbation and mitochondrial iron assembly under H/R (Fig. 5 C and D). It can be inferred that ferroptosis inhibition is crucial to the protective effect of ozone in the H/R model. By virtue of the increase in Gpx4 and Slc7a11 levels by ozone leading to ferroptosis inhibition and corresponding with Nrf2-inducing antioxidant enzymes, we hypothesized that the possible mechanism underlying the protective effect of ozone was likely to be the Nrf2-Slc7a11-Gpx4 interaction.

As an antioxidant transcription factor, Nrf2 can be attached to Are and can regulate a variety of antioxidant enzymes to counteract oxidative stress injury [41]. Notably, upregulating Nrf2 can diminish cardiac dysfunction and antagonize remodeling in metabolic syndrome induced by diet [42]. In addition, loss of Nrf2 can lead to cardiac hypertrophy as well as left ventricular diastolic dysfunction [43]. Nrf2 functions in a complex system based on nuclear translocation and protein turnover, with Keap1 being one of its major regulators [44,45]. Keap1 can form conjugates with Nrf2, prompting ubiquitination of Nrf2 and

proteasome-dependent degradation. Among the canonical pathways regulated by Nrf2, Keap1 is inactivated after oxidation of reactive cysteine residues, resulting in the dissociation of Nrf2 from Keap1, which allows stable transfer of Nrf2 to the nucleus for the next step of transcription [43]. It is demonstrated by this study that ozone administration releases the Keap1-Nrf2 interaction as well as Nrf2 nuclear translocation, which enhances downstream antioxidant enzyme levels. *In vitro*, it was recapitulated that Nrf2 nuclear translocation and downstream antioxidant induction were enhanced by ozone (Fig. 4). The loss of function study caused by SiNrf2 indicates that Nrf2 serves eminently in the ozone protection of HR injury (Fig. 6).

5. Conclusion

Based on our research, we can conclude that ozone has potential value as an adjuvant therapy for treating ischemic heart disease. In addition, our study specifically demonstrated the role of the Nrf2/Slc7a11/Gpx4 signaling axis in the process by which ozone protects the myocardium from ischemia—reperfusion (I/R) injury (Fig. 7). However, *in vitro* experiments still have some limitations, and further studies in clinical settings are necessary to verify the therapeutic effect of ozone.

Author statement

Zhouquan Wu and Liang Zhu provided the experimental ideas of this study and reviewed and revised the first draft of the manuscript. Shengyang Ding and Xinyu Duanmu did the data collection and verified by Lingshan Xu. Shengyang Ding did the data analysis, visualization of results, and wrote the first draft of the manuscript. All authors contributed to the article and approved the submitted version.

Funding

This study was supported by Jiangsu Administration of Traditional Chinese Medicine (MS2021055) and Jiangsu Medical Association (SYH-32021-0041).

Declaration of Competing Interest

The authors declared no potential conflicts of interest with respect to

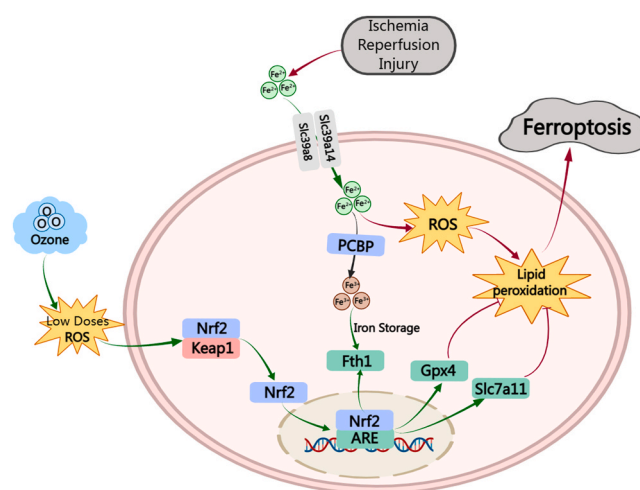


Fig. 7. : Ozone pretreatment can alleviate myocardial ferroptosis caused by ischemia reperfusion injury. Ischemia-reperfusion leads to myocardial damage and ferroptosis by increasing the levels of mitochondria ferrous ions aggregation, reactive oxygen species, and lipid peroxidation. Ozone pretreatment activates the Nrf2/Slc7a11/Gpx4 axis, enhances the myocardial ability to resist oxidative stress injury, and alleviates ferroptosis caused by mitochondria ferrous ion aggregation in myocardial cells.

the research, author-ship, and publication of this article.

References

- [1] M. Ashraf, M. Ebner, C. Wallner, M. Haller, S. Khalid, H. Schwelberger, K. Koziel, M. Enthammer, M. Hermann, S. Sickinger, et al., A p38mapk/mk2 signaling pathway leading to redox stress, cell death and ischemia/reperfusion injury, *Cell Commun. Signal.: CCS* 12 (2014) 6.
- [2] S. Hernandez-Resendiz, K. Chinda, S. Ong, H. Cabrera-Fuentes, C. Zazueta, D. Hausenloy, The role of redox dysregulation in the inflammatory response to acute myocardial ischaemia-reperfusion injury - adding fuel to the fire, *Curr. Med. Chem.* 25 (2018) 1275–1293.
- [3] H. Zhou, J. Wang, P. Zhu, S. Hu, J. Ren, Ripk3 regulates cardiac microvascular reperfusion injury: the role of ip3r-dependent calcium overload, xo-mediated oxidative stress and F-actin/filopodia-based cellular migration, *Cell. Signal.* 45 (2018) 12–22.
- [4] K. Shanmugam, S. Ravindran, G. Kurian, M. Rajesh, Bfisetin confers cardioprotection against myocardial ischemia reperfusion injury by suppressing mitochondrial oxidative stress and mitochondrial dysfunction and inhibiting glycogen synthase kinase 3 activity, *Oxid. Med. Cell. Longev.* 2018 (2018) 9173436.
- [5] W. Li, G. Feng, J. Gauthier, I. Lokshina, R. Higashikubo, S. Evans, X. Liu, A. Hassan, S. Tanaka, M. Cicka, et al., Ferroptotic cell death and thr4/trif signaling initiate neutrophil recruitment after heart transplantation, *J. Clin. Investig.* 129 (2019) 2293–2304.
- [6] X. Fang, H. Wang, D. Han, E. Xie, X. Yang, J. Wei, S. Gu, F. Gao, N. Zhu, X. Yin, et al., Ferroptosis as a target for protection against cardiomyopathy, *Proc. Natl. Acad. Sci. USA* 116 (2019) 2672–2680.
- [7] M. Galiè, V. Covi, G. Tabaracci, M. Malatesta, The role of nrf2 in the antioxidant cellular response to medical ozone exposure, *Int. J. Mol. Sci.* 20 (2019).
- [8] V. Bocci, Scientific and medical aspects of ozone therapy. State of the art, *Arch. Med. Res.* 37 (2006) 425–435.
- [9] Z. Wang, A. Zhang, W. Meng, T. Wang, D. Li, Z. Liu, H. Liu, Ozone protects the rat lung from ischemia-reperfusion injury by attenuating nlrp3-mediated inflammation, enhancing nrf2 antioxidant activity and inhibiting apoptosis, *Eur. J. Pharmacol.* 835 (2018) 82–93.
- [10] W. Meng, Y. Xu, D. Li, E. Zhu, L. Deng, Z. Liu, G. Zhang, H. Liu, Ozone protects rat heart against ischemia-reperfusion injury: a role for oxidative preconditioning in attenuating mitochondrial injury, *Biomed. Pharmacother.* 88 (2017) 1090–1097.
- [11] G. Martínez-Sánchez, S. Al-Dalain, S. Menéndez, L. Re, A. Giuliani, E. Candelario-Jalil, H. Alvarez, J. Fernández-Montequín, O. León, Therapeutic efficacy of ozone in patients with diabetic foot, *Eur. J. Pharmacol.* 523 (2005) 151–161.
- [12] B. Stockwell, Friedmann Angeli, J. Bayir, H. Bush, A. Conrad, M. Dixon, S. Fulda, S. Gascón, S. Hatzios, S. Kagan, Ferroptosis: a regulated cell death nexus linking metabolism, redox biology, and disease, *Cell* 171 (2017) 273–285.
- [13] S. Dixon, K. Lemberg, M. Lamprecht, R. Skouta, E. Zaitsev, C. Gleason, D. Patel, A. Bauer, A. Cantley, W. Yang, et al., Ferroptosis: an iron-dependent form of nonapoptotic cell death, *Cell* 149 (2012) 1060–1072.
- [14] K. Bell, B. Al-Mubarak, J. Fowler, P. Baxter, K. Gupta, T. Tsujita, S. Chowdhry, R. Patani, S. Chandran, K. Horsburgh, et al., Mild oxidative stress activates nrf2 in astrocytes, which contributes to neuroprotective ischemic preconditioning, *Proc. Natl. Acad. Sci. USA* 108 (2011) E1–E2, author reply E3–4.
- [15] D. Szklarczyk, J. Morris, H. Cook, M. Kuhn, S. Wyder, M. Simonovic, A. Santos, N. Doncheva, A. Roth, P. Bork, et al., The string database in 2017: quality-controlled protein-protein association networks, made broadly accessible, *Nucleic Acids Res.* 45 (2017) D362–D368.
- [16] X. Wu, Y. Qin, X. Zhu, D. Liu, F. Chen, S. Xu, D. Zheng, Y. Zhou, J. Luo, Increased expression of dram1 confers myocardial protection against ischemia via restoring autophagy flux, *J. Mol. Cell. Cardiol.* 124 (2018) 70–82.
- [17] X. Wu, L. He, Y. Cai, G. Zhang, Y. He, Z. Zhang, X. He, Y. He, G. Zhang, J. Luo, Induction of autophagy contributes to the myocardial protection of valsartan against ischemia-reperfusion injury, *Mol. Med. Rep.* 8 (2013) 1824–1830.
- [18] L. Xu, L. Zhu, P. Liu, Z. Wu, Z. Zou, Ozone induces tolerance against cardiomyocytes oxygen-glucose deprivation/reperfusion through inhibition of autophagy pathway, *Exp. Ther. Med.* 22 (2021) 869.
- [19] D. Zheng, Z. Liu, Y. Zhou, N. Hou, W. Yan, Y. Qin, Q. Ye, X. Cheng, Q. Xiao, Y. Bao, et al., Urolithin b, a gut microbiota metabolite, protects against myocardial ischemia/reperfusion injury via p62/keap1/nrf2 signaling pathway, *Pharmacol. Res.* 153 (2020), 104655.
- [20] W. Zhang, Y. Sun, L. Bai, L. Zhi, Y. Yang, Q. Zhao, C. Chen, Y. Qi, W. Gao, W. He, et al., Rbms1 regulates lung cancer ferroptosis through translational control of sic7a11, *J. Clin. Investig.* (2021) 131.
- [21] D. Wu, Q. Hu, Y. Wang, M. Jin, Z. Tao, J. Wan, Identification of hmx1 as a critical ferroptosis-related gene in atherosclerosis, *Front. Cardiovasc. Med.* 9 (2022), 833642.
- [22] F. Gao, Y. Zhao, B. Zhang, C. Xiao, Z. Sun, Y. Gao, X. Dou, Suppression of Incrna gm47283 attenuates myocardial infarction via mir-706/ ptps2/ferroptosis axis, *Bioengineered* 13 (2022) 10786–10802.
- [23] E. Son, D. Lee, C.W. Woo, Y.H. Kim, The optimal model of reperfusion injury in vitro using h9c2 transformed cardiac myoblasts, *Korean J. Physiol. Pharm.* 24 (2020) 173–183.
- [24] M. Dodson, R. Castro-Portuguez, D. Zhang, Nrf2 plays a critical role in mitigating lipid peroxidation and ferroptosis, *Redox Biol.* 23 (2019), 101107.
- [25] T. Kalogeris, Y. Bao, R. Korhuis, Mitochondrial reactive oxygen species: a double edged sword in ischemia/reperfusion vs preconditioning, *Redox Biol.* 2 (2014) 702–714.
- [26] J. Kim, Y. Jin, J. Lemasters, Reactive oxygen species, but not ca2+ overloading, trigger ph- and mitochondrial permeability transition-dependent death of adult rat myocytes after ischemia-reperfusion, *Am. J. Physiol. Heart Circ. Physiol.* 290 (2006) H2024–H2034.
- [27] A. Perricone, R. Vander Heide, Novel therapeutic strategies for ischemic heart disease, *Pharmacol. Res.* 89 (2014) 36–45.
- [28] E. Son, D. Lee, C. Woo, Y. Kim, In vitro the optimal model of reperfusion injury using h9c2 transformed cardiac myoblasts, *Korean J. Physiol. Pharmacol.: Off. J. Korean Physiol. Soc. Korean Soc. Pharmacol.* 24 (2020) 173–183.
- [29] V. Bocci, E. Borrelli, V. Travagli, I. Zanardi, The ozone paradox: ozone is a strong oxidant as well as a medical drug, *Med. Res. Rev.* 29 (2009) 646–682.
- [30] M. Muto, F. Giurazza, R. Silva, G. Guarnieri, Rational approach, technique and selection criteria treating lumbar disk herniations by oxygen-ozone therapy, *Interv. Neuroradiol.: J. Peritherapeutic Neuroradiol., Surg. Proced. Relat. Neurosci.* 22 (2016) 736–740.
- [31] A. Aslaner, T. Çakır, S. Tekeli, S. Avcı, U. Doğan, F. Tekeli, H. Soylu, C. Akyüz, S. Koç, I. Üstünel, et al., Medical ozone treatment ameliorates the acute distal colitis in rat, *Acta Cir. Bras.* 31 (2016) 256–263.
- [32] N. Santana-Rodríguez, P. Llontop, B. Clavo, M. Fiuza-Pérez, K. Zerecero, A. Ayub, K. Alshehri, N. Yordi, L. Re, W. Raad, et al., Ozone therapy protects against rejection in a lung transplantation model: a new treatment? *Ann. Thorac. Surg.* 104 (2017) 458–464.
- [33] M. Izadi, M. Bozorgi, M. Hosseini, N. Khalili, N. Jonaidi-Jafari, Health-related quality of life in patients with chronic wounds before and after treatment with medical ozone, *Medicine* 97 (2018), e12505.
- [34] A. Isik, K. Peker, C. Gursul, I. Sayar, D. Firat, I. Yilmaz, I. Demiryilmaz, The effect of ozone and naringin on intestinal ischemia/reperfusion injury in an experimental model, *Int. J. Surg.* 21 (2015) 38–44.
- [35] M. Luongo, A. Brigida, L. Mascolo, G. Gaudino, Possible therapeutic effects of ozone mixture on hypoxia in tumor development, *Anticancer Res.* 37 (2017) 425–435.
- [36] L. Amin, Biological assessment of ozone therapy on experimental oral candidiasis in immunosuppressed rats, *Biochem. Biophys. Rep.* 15 (2018) 57–60.
- [37] S. Isler, B. Unsal, F. Soysal, G. Ozcan, E. Peker, I. Karaca, The effects of ozone therapy as an adjunct to the surgical treatment of peri-implantitis, *J. Periodontal Implant Sci.* 48 (2018) 136–151.
- [38] W. Pryor, B. Das, D. Church, The ozonation of unsaturated fatty acids: aldehydes and hydrogen peroxide as products and possible mediators of ozone toxicity, *Chem. Res. Toxicol.* 4 (1991) 341–348.
- [39] Y. Zhao, Y. Li, R. Zhang, F. Wang, T. Wang, Y. Jiao, The role of erastin in ferroptosis and its prospects in cancer therapy, *OncoTargets Ther.* 13 (2020) 5429–5441.
- [40] P. Liu, Y. Feng, H. Li, X. Chen, G. Wang, S. Xu, Y. Li, L. Zhao, Ferrostatin-1 alleviates lipopolysaccharide-induced acute lung injury via inhibiting ferroptosis, *Cell. Mol. Biol. Lett.* 25 (2020) 10.
- [41] S. Cadenas, Ros and redox signaling in myocardial ischemia-reperfusion injury and cardioprotection, *Free Radic. Biol. Med.* 117 (2018) 76–89.
- [42] S. Panchal, L. Ward, L. Brown, Ellagic acid attenuates high-carbohydrate, high-fat diet-induced metabolic syndrome in rats, *Eur. J. Nutr.* 52 (2013) 559–568.
- [43] R. Erkens, C. Kramer, W. Lückstädt, C. Panknin, L. Krause, M. Weidenbach, J. Dirzka, T. Krenz, E. Mergia, T. Suvorava, et al., Left ventricular diastolic dysfunction in nrf2 knock out mice is associated with cardiac hypertrophy, decreased expression of serca2a, and preserved endothelial function, *Free Radic. Biol. Med.* 89 (2015) 906–917.
- [44] C. Silva-Islas, P. Maldonado, Canonical and non-canonical mechanisms of nrf2 activation, *Pharmacol. Res.* 134 (2018) 92–99.
- [45] V. Krajka-Kuźniak, J. Paluszczak, W. Baer-Dubowska, The nrf2-are signaling pathway: an update on its regulation and possible role in cancer prevention and treatment, *Pharmacol. Rep.: PR* 69 (2017) 393–402.